

The linear stability of high-frequency flow in a torsionally oscillating cylinder

P. J. BLENNERHASSETT¹ AND ANDREW P. BASSOM²

¹School of Mathematics, University of New South Wales, Sydney 2052, Australia

²School of Mathematics and Statistics, University of Western Australia,
Crawley 6009, Australia

(Received 24 January 2006 and in revised form 21 November 2006)

The linear stability of the Stokes layer induced in a fluid contained within a long cylinder oscillating at high frequency about its longitudinal axis is investigated. The disturbance equations are derived using Floquet theory and the resulting system solved using pseudo-spectral methods. Both shear modes and axially periodic centripetal disturbance modes are examined and neutral stability curves and corresponding critical conditions for instability identified. For sufficiently small cylinder radius it is verified that the centripetal perturbations limit the stability of the motion but that in larger-radius configurations the shear modes associated with the Stokes layer take over this role. These results suggest a possible design, free of entry-length effects, for experiments intended to examine the breakdown of oscillatory boundary layers.

1. Introduction

The stability of time-periodic laminar flows is a topic of long-standing theoretical and practical importance. A paradigm for many types of oscillatory flow is the flat Stokes layer, which is itself one of the relatively few exact solutions of the incompressible Navier–Stokes equations. While there is overwhelming experimental evidence that this flow is unstable, only relatively recently has there been any self-consistent theoretical analysis which suggests this is the case. A number of early studies, for example those by von Kerczek & Davis (1974) or Hall (1978), were constrained by computational issues that meant they were only able to access parameter regimes in which the flow is linearly stable. Blondeaux & Seminara (1979) used a slowly varying approximation to conclude that at relatively modest Reynolds numbers the Stokes layer might be unstable over parts of the oscillation close to flow reversal, although, over the complete cycle, perturbations experience net decay. The first report of a neutral stability curve, in the usual Reynolds number–wavenumber parameter space, appears to be that of Blennerhassett & Bassom (2002), hereafter referred to as BB02. There we used a semi-analytical method first proposed by Seminara & Hall (1976), who were concerned with the centrifugal stability of curved Stokes layers, and later adapted by Hall (1978) for the flat Stokes layer problem. In BB02 we were able to find a critical Reynolds number for the instability of the flow induced by an oscillating plate bounding a semi-infinite layer of fluid. A subsequent investigation (Blennerhassett & Bassom 2006) (BB06) has extended this work to examine the stability of oscillatory flows within a finite-gap channel and in a circular pipe. The linear disturbance equations were solved using Floquet theory and pseudo-spectral numerical techniques and the earlier results of BB02 retrieved in appropriate wide-channel limits.

One difficulty commented upon in both BB02 and BB06 is the large discrepancy between the theoretical predictions and experimental observations of the onset of instability in flat Stokes layers. Details of various experimental results are described in both those papers but, in brief, many practical realizations of the instability suggest that onset occurs at a Reynolds number less than one half that predicted by linear theory. An indication of the difficulties associated with these experiments is that there is still no agreed definite value for the transition Reynolds number, as there is significant variation in the results obtained by different researchers. Several reasons for the discrepancies between theory and experiment have been proposed. An analytical study by Blondeaux & Vittori (1994) and numerical simulations by Spalart & Baldwin (1988), Verzicco & Vittori (1996) and Vittori & Verzicco (1998) have suggested that wall imperfections or other external sources might play important roles in triggering the appearance of turbulence in oscillatory flows. Blondeaux & Vittori (1994) used a two-dimensional analysis to show that the flow deviates from the laminar regime because of the growth of perturbations during certain phases of the oscillation cycle; the origin of this phenomenon lies in a resonance effect. Further simulations by Akhavan, Kamm & Shapiro (1991) showed that, at sufficiently high Reynolds numbers, three-dimensional disturbances can grow on pre-existing two-dimensional waves. By way of an alternative, Wu (1992) proved how a resonant triad mechanism operating between a certain two-dimensional wave and a pair of three-dimensional modes can lead to a finite-time singularity. The direct numerical simulations of Vittori & Verzicco (1998) seem to indicate that the Akhavan *et al.* (1991) process is the likelier in practice, and recent calculations by Costamagna, Vittori & Blondeaux (2003) throw light on more strongly nonlinear aspects of transition. It should be noted that the work described above was probably carried out under the conjecture, expressed most strongly by Yang & Yih (1977), that the flat Stokes layer is linearly stable. While the results summarized above will continue to have relevance, the linear instability predictions in BB02 and BB06 allow alternative interpretations of the existing experimental results.

Another possibility for the wide variation between the theory and experimental observations of the onset of instability in flat Stokes layers is that in practice it is hard to ensure that disturbances remain strictly within the scope of linear theory. Further, oscillating flows in channels or pipes are usually generated by a combination of an oscillating piston and a contraction in the flow. The underlying assumption is that, sufficiently far from the piston or the contraction, any disturbances caused by this device will decay leaving a velocity profile close to that appropriate to an infinitely long channel or pipe. However, one implication of the results described in BB06 is that as critical conditions are approached the spatial decay of disturbances becomes increasingly weak and the influence of the piston or contraction extends further and further into the flow. This behaviour, combined with the acknowledgment that conducting low-background-noise experiments in long oscillating channels or pipes is far from easy, is a motivating factor for the work to be described here. It is hoped that better agreement between theoretical predictions and experimental measurements of the stability of oscillatory shear layers could be achieved in a closed system free of the effects of a driving piston. Thus we proposed to study the linear instability of shear modes present in the Stokes layer induced in a fluid contained within a torsionally oscillating long circular cylinder.

The calculations presented here allow incorporation of the effects of curvature on the stability of the flat oscillating layers studied in BB02 and BB06, although the curved geometry means that centripetal instability could also be present in the system.

Seminara & Hall (1976) investigated the stability of the Stokes layer generated on an infinitely long cylinder that oscillates harmonically about its longitudinal axis while immersed in an unbounded viscous fluid. In such a flow, instability appears as axisymmetric Taylor vortices which are periodic in the axial direction. A similar mechanism is operative in the problem studied by Papageorgiou (1987) who was concerned with the stability of oscillatory flow through a curved pipe. Here the flow was driven by a sinusoidal pressure gradient and the instability appeared on the outer bend of the pipe. Both these centripetal instability mechanisms require significant curvature in the flow streamlines and it is therefore likely that for large enough cylinders the flow considered in our work will be more susceptible to a shear-mode instability than to centripetally induced structures. To determine which disturbance form defines the linear instability of the flow, both types will be examined.

The remainder of this study is laid out as follows. The governing linear stability equations are derived in §2, where the numerical methods are also outlined. The results for both shear and centripetal modes are discussed in §3, which is followed by a few final remarks.

2. Formulation and numerical methods

Consider the motion induced in a Newtonian fluid (of kinematic viscosity ν) within an infinitely long circular cylinder of radius r_o by oscillating it about its longitudinal axis with frequency ω . If there are no disturbances then a unidirectional azimuthal flow is generated. A dimensionless form for this basic flow is obtained if all lengths are scaled on $\sqrt{2\nu/\omega}$, all velocity components on V_0 , the amplitude of the velocity oscillations, and a non-dimensional time $\tau = \omega t$ is introduced. In standard cylindrical polar coordinates (r, θ, z) the undisturbed basic flow takes the form

$$\begin{aligned}
 v &= V_B(r, \tau) = \text{Re} \left\{ \frac{J_1((1-i)r)}{J_1((1-i)H)} e^{i\tau} \right\} \\
 &= v_1(r)e^{i\tau} + v_{-1}(r)e^{-i\tau}, \quad u = w = 0, \quad 0 \leq r \leq H,
 \end{aligned}
 \tag{2.1}$$

where the velocity vector $\mathbf{u} = (u, v, w)$ has components corresponding to the coordinates (r, θ, z) and J_1 is the Bessel function of order unity. The non-dimensional radius of the cylinder is $H \equiv r_o \sqrt{\omega/2\nu}$.

For large values of H it is expected that the basic flow (2.1) will approximate that of a flat plate oscillating in its own plane and bounding a semi-infinite layer of fluid. The linear stability of this planar basic flow was examined in BB02 by looking for disturbances in the form of two-dimensional waves, periodic in the direction of oscillation of the bounding plate and travelling in that direction. Here we first consider the linear stability of the basic flow (2.1) to two-dimensional travelling-wave perturbations analogous to those of the planar geometry of BB02. Thus the perturbations considered initially will have azimuthal and radial velocity components only, corresponding to velocity components parallel and normal to the oscillating bounding surface.

The perturbed basic flow having the structure described above can be expressed in the form

$$(u, v, w) = (0, V_B, 0) + \varepsilon \left(\frac{1}{r} \frac{\partial \Psi}{\partial \theta}, -\frac{\partial \Psi}{\partial r}, 0 \right),
 \tag{2.2}$$

where $\varepsilon \ll 1$ and Ψ denotes the stream function of a two-dimensional disturbance. The stream function Ψ is now decomposed to expose explicitly the periodicity of the perturbation in the azimuthal direction and any exponential growth with time. As the basic flow is periodic in time, $\Psi(r, \theta, \tau)$ must have a Floquet structure and hence has the form

$$\Psi = e^{\mu\tau} e^{iq\theta} \psi(r, \tau) + \text{complex conjugate}, \tag{2.3}$$

where $\psi(r, \tau)$ is taken to be 2π -periodic in τ , any exponential growth or decay of Ψ being incorporated in μ ; the azimuthal wavenumber q is necessarily an integer. With the velocity field given by (2.2) and (2.3) the linearized equation for ψ is then

$$\frac{\partial}{\partial \tau} \mathcal{L}_q \psi = \left\{ \frac{1}{2} \mathcal{L}_q - \mu - \frac{iqR}{r} V_B \right\} \mathcal{L}_q \psi + \frac{iqR}{r} \psi \mathcal{L}_1 V_B, \tag{2.4}$$

where the operator \mathcal{L}_q is defined by

$$\mathcal{L}_q \equiv \frac{\partial^2}{\partial r^2} + \frac{1}{r} \frac{\partial}{\partial r} - \frac{q^2}{r^2}$$

and the Reynolds number R , which is the main parameter determining the stability of the flow, is given by

$$R = \frac{V_0}{\sqrt{2\nu\omega}}.$$

(This form for R , effectively based on the characteristic length $\frac{1}{2}\sqrt{2\nu/\omega}$, removes some factors of one half from the linear stability equation (2.4).)

Equation (2.4) needs to be solved subject to the usual no-slip boundary conditions

$$\psi = \psi_r = 0 \quad \text{on} \quad r = H, \tag{2.5}$$

together with suitable regularity requirements at the origin $r = 0$. The growth rate μ is complex, while the time symmetries of the equation allow all solutions to be obtained by restricting the imaginary part of μ to the interval $\mu_i \in [0, \frac{1}{2}]$, as described in BB02. The unknown function ψ is decomposed into harmonics,

$$\psi = \sum_{n=-\infty}^{\infty} \psi_n(r) e^{in\tau}, \tag{2.6}$$

so that equating coefficients of the harmonics in (2.4) results in the infinite system of ordinary differential equations

$$(\mathcal{L}_q - 2\mu - 2in)\mathcal{L}_q \psi_n = \frac{2iqR}{r} [(\mathcal{L}_q \psi_{n-1} - 2i\psi_{n-1})v_1 + (\mathcal{L}_q \psi_{n+1} + 2i\psi_{n+1})v_{-1}]. \tag{2.7}$$

The numerical solution of the system (2.7) was obtained using the pseudo-spectral techniques described by Fornberg (1996) and Trefethen (2000). Analogous methods were used in BB06 so here only the key steps in the numerical procedures are presented and the important differences highlighted. Each differential operator appearing in the governing equations (2.7) was replaced by its pseudo-spectral matrix approximation, with each $\psi_n(y)$ being represented by a vector $\boldsymbol{\psi}_n$ of its function values at the computational grid points. As is usual in pseudo-spectral methods, the problem was solved on a Chebyshev mesh, here containing $2K + 1$ points and spanning the interval $-H \leq r \leq H$. Thus a discrete approximation to the equations (2.7) can be written as

$$-iqR\tilde{M}\boldsymbol{\psi}_{n+1} + (\mathbf{L}^{-1}\mathbf{V} - in\mathbf{I})\boldsymbol{\psi}_n - iqR\mathbf{M}\boldsymbol{\psi}_{n-1} = \mu\boldsymbol{\psi}_n, \tag{2.8}$$

for each integer n . Here I is the appropriately sized identity matrix and L , V and M are pseudo-spectral differentiation matrices representing the continuous operators listed:

$$\mathcal{L}_q \rightarrow L, \quad \mathcal{L}_q^2 \rightarrow 2V \quad \text{and} \quad M = L^{-1}(r^{-1}v_1(L - 2iI)). \tag{2.9}$$

Finally, \tilde{M} denotes the complex conjugate of M and, allowing for an obvious abuse of notation, v_1 and r^{-1} in (2.9) denote square matrices with the mesh values of $v_1(r)$ and r^{-1} down the diagonal. Note that for the domain $-H \leq r \leq H$ the quantity $r^{-1}v_1(r)$ is an even function of r and is bounded as $r \rightarrow 0$.

For calculating the stability of the flow the computational domain $-H \leq r \leq H$ was reduced to $0 \leq r \leq H$ by exploiting the symmetries of the stream function $\psi_n(r)$. For even integer wavenumbers q the stream function is even in r while $\psi_n(r)$ is odd in r when q is odd. Appropriate kinematic conditions (Batchelor & Gill 1962) were then imposed at the origin and the usual no-slip requirements applied at the boundary $r = H$ (see BB06). A finite system of equations was obtained by truncating the Fourier series (2.6) for ψ and setting $\psi_n = 0$ for $|n| > N$, where N needs to be typically 200–300 to locate neutral conditions. The system (2.8) then can be written as an algebraic eigenvalue problem

$$A\Phi = \mu\Phi \tag{2.10}$$

where A is a sparse, block diagonal matrix and the vector Φ is given by

$$\Phi^T = (\psi_N^T \quad \psi_{N-1}^T \quad \cdots \quad \psi_0^T \quad \cdots \quad \psi_{-N}^T). \tag{2.11}$$

The eigenvalues μ and eigenvectors Φ of this problem were found using the sparse-matrix eigenvalue routines in Matlab. Checks on the consistency and accuracy of the eigenvalue μ and the eigenfunctions ψ_n similar to those in BB06 were carried out and the interested reader is directed to that paper for further details. In particular, the main difficulty that had to be overcome was the appearance of numerical noise in the large- n eigenfunctions when N was greater than about 120. As in BB06, a rescaling of the eigenfunctions ψ_n that accounted for the exponential decay of these Fourier coefficients removed the unwanted noise and enabled efficient calculation of the eigenvalue to at least eight significant figures over a wide range of parameter space.

When conducting the numerical work it was found that to maintain the accuracy of the solutions the number of points in the Chebyshev mesh had to increase as H increased, thereby causing the run time of the codes to grow markedly. However, the main activity of the disturbance was seen to be concentrated relatively close to the oscillating cylinder with essentially no disturbance present around the centre of the cylinder, suggesting that it is only the region close to the boundary that needed accurate numerical resolution. Indeed, BB06 found that the critical conditions for the instability of oscillatory flow in a channel are effectively the same as those for the flow of a semi-infinite layer of fluid overlying an oscillating plate, provided that the channel half-width is at least 16 times the Stokes layer thickness. Accordingly, although the geometry inherent in the basic flow (2.1) is the primary focus of our work, it proved computationally convenient to consider instead the oscillatory flow in an annular domain $h \leq r \leq H$, where the non-dimensional radius of the inner bounding cylinder is defined as $h \equiv r_i \sqrt{\omega/2\nu}$. In this configuration the basic flow

generated by oscillating the outer cylinder, with the inner cylinder fixed, is given by

$$v = V_B(r, \tau) = \text{Re} \left\{ \frac{H_1^{(1)}((1-i)h)H_1^{(2)}((1-i)r) - H_1^{(2)}((1-i)h)H_1^{(1)}((1-i)r)}{H_1^{(1)}((1-i)h)H_1^{(2)}((1-i)H) - H_1^{(2)}((1-i)h)H_1^{(1)}((1-i)H)} e^{i\tau} \right\}, \quad (2.12a)$$

$$u = w = 0, \quad h \leq r \leq H, \quad (2.12b)$$

where $H_1^{(1)}$ and $H_1^{(2)}$ denote order-one Hankel functions of the first and second kind, respectively. In passing, we remark that although it is possible to write (2.12) in terms of other special functions, the attraction of the Hankel function is that it exhibits explicitly the exponential decay of the basic flow away from the outer cylinder.

The use of the annular basic flow (2.12) required a few changes in the details of the numerical scheme described above. As the domain of interest no longer extends to the origin, the regularity requirements at $r = 0$ in the full cylinder calculations are replaced by the no-slip conditions $\psi = \psi_r = 0$ on $r = h$ (cf. (2.5)). Further, the Chebyshev mesh now covers only $h \leq r \leq H$ and the distinction between even and odd wavenumbers q is no longer relevant as there was no need to invoke any symmetry properties of $\psi_n(r)$. In all other respects the numerical strategy is unchanged.

Tests were carried out to determine when the stability properties of the annular basic flow (2.12) constituted an accurate approximation to those of the basic flow in the cylinder (2.1) for the case of the shear-mode disturbances considered thus far. Some details of these tests will be given in §3, but the main result was that provided $H - h > 16$ the stability characteristics of the two basic flows were essentially the same for all $H > 16$. This conclusion is in line with the findings of BB06 and allowed the stability properties of the full cylinder flow to be calculated more efficiently via an annular-flow problem.

2.1. Centripetal modes

Previous analysis of centripetal instability in oscillatory flow (Seminara & Hall 1976; Riley & Laurence 1976; Papageorgiou 1987) focused on finding a critical Taylor number for instability. Such calculations contain the implied limit of large Reynolds numbers and hence are not strictly relevant to the finite- R flow considered here. Thus, for the case of centripetally unstable perturbations to the basic flow (2.1), the derivation of the disturbance equations follows the argument for the shear modes described above rather than the traditional narrow-gap Taylor-limit argument used by Riley & Laurence (1976). Briefly, the disturbed flow is taken to be axisymmetric and to have the structure

$$(u, v, w) = (0, V_B, 0) + \varepsilon \left(\frac{1}{r} \frac{\partial \Psi}{\partial z}, \tilde{v}, -\frac{1}{r} \frac{\partial \Psi}{\partial r} \right). \quad (2.13)$$

The assumption of a Floquet decomposition in the form

$$(\Psi, \tilde{v}) = e^{\mu\tau} e^{iaz} (\psi(r, \tau), \phi(r, \tau)) + \text{complex conjugate}, \quad (2.14)$$

where both ψ and ϕ are 2π -periodic in τ , results in the governing equations

$$\mathcal{M}_a \psi_\tau + \mu \mathcal{M}_a \psi - 2iaRV_B \phi = \frac{1}{2} \mathcal{M}_a^2 \psi, \quad (2.15a)$$

$$\phi_\tau + \mu \phi + iar^{-2} R(rV_B)_r \psi = \frac{1}{2} (\mathcal{M}_a \phi + 2r^{-1} \phi_r - r^{-2} \phi), \quad (2.15b)$$

where $\mathcal{M}_a \equiv \partial_r^2 - r^{-1}\partial_r - a^2$. When ψ and ϕ are decomposed into their Fourier components,

$$(\psi(r, \tau), \phi(r, \tau)) = \left(\sum_{n=-\infty}^{\infty} \psi_n(r) e^{in\tau}, \sum_{n=-\infty}^{\infty} \phi_n(r) e^{in\tau} \right) \tag{2.16}$$

and like powers of $e^{i\tau}$ collected in system (2.15), the governing equations in the frequency domain become

$$(in + \mu)\mathcal{M}_a \psi_n - 2iaR(v_{-1}\phi_{n+1} + v_1\phi_{n-1}) = \frac{1}{2}\mathcal{M}_a^2 \psi_n, \tag{2.17a}$$

$$(in + \mu)\phi_n + iar^{-2}R((rv_{-1})_r \psi_{n+1} + (rv_1)_r \psi_{n-1}) = \frac{1}{2}(\mathcal{M}_a \phi_n + 2r^{-1}\phi_{nr} - r^{-2}\phi_n). \tag{2.17b}$$

These equations need to be solved subject to the requirements that $\psi_n = \psi_{nr} = \phi_n = 0$ on $r = H$ and suitable regularity conditions at the origin $r = 0$.

The numerical solution of the system (2.17) was obtained using pseudo-spectral techniques analogous to those used for the solution of (2.7). Here each $\psi_n(r)$ and each $\phi_n(r)$ was represented by a vector of function values ψ_n or ϕ_n on a suitable Chebyshev mesh. Each differential operator appearing in (2.17) was replaced by its pseudo-spectral matrix approximation, and with Φ now defined as

$$\Phi^T = (\psi_N^T \quad \psi_{N-1}^T \quad \cdots \quad \psi_0^T \quad \cdots \quad \psi_{-N}^T \quad \phi_N^T \quad \phi_{N-1}^T \quad \cdots \quad \phi_0^T \quad \cdots \quad \phi_{-N}^T) \tag{2.18}$$

the system (2.17) can be written as an algebraic eigenvalue problem

$$\mathbf{B}\Phi = \mu\Phi \tag{2.19}$$

where \mathbf{B} is a sparse, block diagonal matrix. The eigenvalues μ and eigenvectors Φ of this problem were again found using Matlab.

The implementation of the above numerical algorithm was checked by solving the equations (2.15) on an annular domain with the basic flow and boundary conditions appropriate to the problem studied by Seminara & Hall (1976). Theoretically, Seminara & Hall (1976) considered an infinitely long cylinder oscillating in an unbounded fluid, but, for both their numerical calculations and their experimental realizations, they actually used an annular region. The basic flow in this domain, with the inner cylinder oscillating and the outer cylinder at rest, is given by

$$v = V_B(r, \tau) = Re \left\{ \frac{H_1^{(1)}((1-i)H)H_1^{(2)}((1-i)r) - H_1^{(2)}((1-i)H)H_1^{(1)}((1-i)r)}{H_1^{(1)}((1-i)H)H_1^{(2)}((1-i)h) - H_1^{(2)}((1-i)H)H_1^{(1)}((1-i)h)} e^{i\tau} \right\}, \tag{2.20a}$$

$$u = w = 0, \quad h \leq r \leq H, \tag{2.20b}$$

which is just (2.12) with h and H interchanged in the expression for v . In Seminara & Hall (1976) the parameter governing the stability of the flow is the Taylor number $T = (2V_0^2/r_i\omega^2)\sqrt{\omega/v}$, as these authors effectively used a narrow-gap approximation based on the small thickness of the Stokes layer compared with the radius of the oscillating cylinder. Expressed in terms of the parameters used here, we have $T = 2\sqrt{2}R^2/h$ and, as the length scales used in the current work and in Seminara & Hall (1976) are identical, the corresponding wavenumber values are also the same. For comparison purposes, a value for the growth rate μ , which is real in this case, is given by Seminara & Hall (1976) as $\mu_{SH} = 0.002\,264\,383$ when $a = 0.858\,52$ and

\sqrt{h}	4	8	16	32
μ	-1.135×10^{-1}	-2.903×10^{-2}	-5.706×10^{-3}	2.669×10^{-4}
\sqrt{h}	64	128	256	512
μ	1.769×10^{-3}	2.145×10^{-3}	2.239×10^{-3}	2.263×10^{-3}

TABLE 1. Values of μ from the solution of (2.17) with the annular basic flow (2.20) as an approximation to the conditions in Seminara & Hall (1976). The wavenumber is $a = 0.858\,52$, the Reynolds number satisfies $R^2 = 165\sqrt{2}h/4$ and $H = h + 16$. The calculations used 64 Chebyshev subintervals in the flow domain and the Fourier series (2.16) only included harmonics with $|n| \leq 10$. In the limit $h \rightarrow \infty$ Seminara & Hall (1976) gives the result $\mu_{SH} = 0.002\,264\,383$.

$T = 165$. The values obtained for μ from the solution of (2.17), with $a = 0.858\,52$, $R^2 = 165\sqrt{2}h/4$ and the basic flow (2.20), are given in table 1.

As reported by Seminara & Hall (1976) only very few harmonics in the Fourier series (2.16) are needed for an accurate numerical solution of the system (2.15). Further, a log-log plot of the difference $\mu_{SH} - \mu$ against h , for the values of μ in table 1, shows that this quantity diminishes like h^{-1} , as should be expected when comparing solutions of the full equations (2.15) with those of the narrow-gap (or Taylor) limit. This check also demonstrates that the Taylor limit of the governing equations provides a good asymptote to the results obtained at finite R .

3. Results

Neutral conditions for the shear modes were obtained by solving system (2.7) with the basic flow (2.1) at fixed values of H and q . The Reynolds number R was varied until the real part of μ satisfied $|\mu_r| < 10^{-3}$. During the iteration an approximation to $d\mu_r/dR$ was calculated and values in the range (0.004, 0.006) were typical, close to neutral conditions. Thus, accepting as zero a value of $O(10^{-3})$ for μ_r results in an error of less than 0.25 in the neutral Reynolds number and, as this quantity is always greater than 700, a relative error of at most 0.04% in the stated neutral R is obtained. At a given value of H this process was repeated for several contiguous integers $q = 2k$ or $q = 2k + 1$, always ensuring that sufficiently many values of q were examined so that a minimum in the value of the neutral Reynolds numbers, as a function of q , could be determined. From this finite set of neutral conditions the value of q with the smallest neutral R was selected to define the critical Reynolds number R_c at the given H . Some results are shown in figure 1, which illustrates the behaviour of the critical Reynolds number for instability, as a function of cylinder radius H , for H up to 50. The curves in figure 1 result from calculations starting at $H = 16$ and incrementing H in steps of 0.2 up to $H = 50$. At the smaller values of H the Fourier series (2.6) was truncated at $N = 400$ and only 112 subintervals were needed in the Chebyshev mesh across the diameter of the cylinder. For the largest H in this figure the number of Chebyshev subintervals on the diameter had to be increased to 176 to maintain adequate resolution of the region occupied by the Stokes layer on the cylinder wall, while the number of Fourier components needed could be reduced to around 250 owing to the reduction in Reynolds number occurring in the calculations.

For a prescribed azimuthal wavenumber q one can envisage a curve of R as a function of H , say $R = R_N(q, H)$, defining neutrally stable conditions for the given

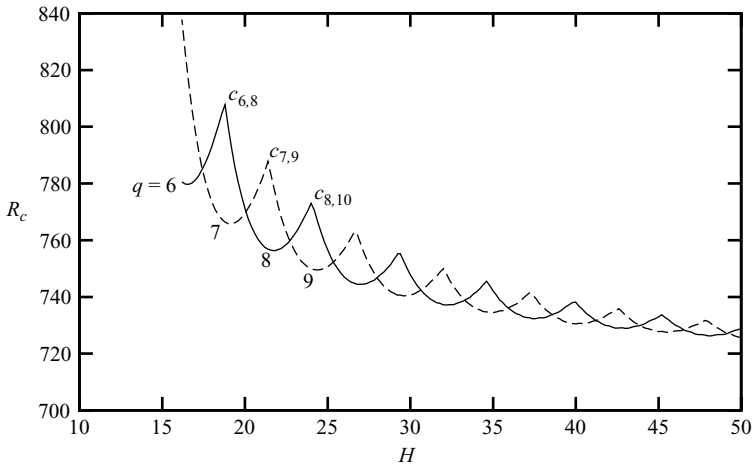


FIGURE 1. Even- and odd-integer-wavenumber critical conditions as a function of H . The even-integer-wavenumber critical conditions are shown by the solid line and the values of the wavenumber q are shown for the first few parabola-like subsections of the critical curve. The dashed line gives the critical conditions for the odd-integer-wavenumber disturbances.

value of q . The solid line in figure 1 is now defined as

$$R = \min_{k \in \mathbb{Z}} R_N(2k, H),$$

so that the point labelled $c_{6,8}$ in this figure is the intersection of the curves $R_N(6, H)$ and $R_N(8, H)$. Similar considerations apply to the critical curve for the odd-integer wavenumbers, shown as the dashed curve in figure 1, and hence the point denoted $c_{7,9}$ lies at the intersection of the curves $R_N(7, H)$ and $R_N(9, H)$.

It is to be expected that each curve $R = R_N(q, H)$ will have a minimum near where the ratio q/H is close to the critical wavenumber for the instability of a Stokes layer on an infinite flat plate. As the critical wavenumber for the flat Stokes layer is fixed at $a_{c\infty} \approx 0.377$ (BB02), the critical azimuthal mode number q must increase as H increases. The overlapping of these individual $R_N(q, H)$ curves for fixed q and increasing H is then the origin of the sawtooth-type profile seen in figure 1.

To access values of $H > 50$ it was computationally more efficient to perform the necessary calculations on an annular domain, the basic flow now being given by (2.12). Following the results of BB06, the inner-cylinder radius h was taken as $h = H - 16$ and the annular gap then was discretized with a Chebyshev mesh of 64 subintervals for all values of H . No-slip boundary conditions were implemented on both the inner and outer cylinders and hence there was no need to use the symmetry or regularity conditions relevant to the cylindrical domain. With the critical conditions for the annular domain determined using the same algorithm as outlined above for the circular domain there was at least four-figure agreement between the two sets of critical Reynolds numbers for $16 < H < 50$. A calculation at $H = 72$ using 224 Chebyshev subintervals in the diameter of the pipe gave a critical R of 721.6671, while the calculation in the annular domain gave 721.6658 for the same outer cylinder radius H . The agreement between these two methods for solving the governing stability equations (2.4) provides an internal check on the implementation of the numerical methods used and confirms the observations in BB06 that a domain wider than 16 Stokes layer thicknesses is effectively infinite as far as the shear-mode linear stability

properties of Stokes layers are concerned. The calculated critical conditions for $H > 50$ will be shown later, along with the critical results for the centripetal modes.

The general trend in the behaviour of R_c , illustrated in figure 1, is as suggested in the introduction: at relatively small cylinder radii the shear modes are less easily excited since it is difficult to achieve a ratio q/H close to a_{∞} , the critical wavenumber for the infinite flat plate, while at large values of H the curvature of the system becomes increasingly less significant and the critical conditions tend to those of the flat Stokes layer. While a large- H asymptote could be calculated, it is of little practical use in predicting which type of disturbance limits the stability of the basic flow (2.1). The same statement holds true for the large- H , or Taylor, limit of (2.15), but for centripetal instabilities the large- H asymptote turns out to be extremely accurate at finite values of H and thus saves considerable computational effort in locating critical conditions for the centripetal instability modes.

The analysis of equations (2.15) for large values of H begins by setting $r = H + \eta$, where $-H \leq \eta \leq 0$, and rescaling the stream function via $\psi \rightarrow (H/R)\psi$. Then in the limit $H \rightarrow \infty$ with the Taylor number $T = R^2/H$ held fixed, the governing system (2.15) reduces to

$$\widehat{\mathcal{M}}_a \psi_\tau + \mu \widehat{\mathcal{M}}_a \psi - 2iaT \widehat{V}_B \phi = \frac{1}{2} \widehat{\mathcal{M}}_a^2 \psi, \quad \phi_\tau + \mu \phi + ia \widehat{V}_{B\eta} \psi = \frac{1}{2} \widehat{\mathcal{M}}_a \phi, \quad (3.1)$$

where $\widehat{\mathcal{M}}_a = \partial_\eta^2 - a^2$, with boundary conditions $\psi = \psi_\eta = \phi = 0$ on $\eta = 0$ and $\psi, \phi \rightarrow 0$ as $\eta \rightarrow -\infty$. In this limit the basic flow (2.1) has the form

$$\widehat{V}_B = e^{(1+i)\eta} e^{i\tau} + e^{(1-i)\eta} e^{-i\tau} = \widehat{v}_1 e^{i\tau} + \widehat{v}_{-1} e^{-i\tau}.$$

A Fourier decomposition of $(\psi(\eta, \tau), \phi(\eta, \tau))$, as in (2.16), reduces the system (3.1) to a problem amenable to the pseudo-spectral solution method developed for the system (2.17). Papageorgiou (1987) showed that the most unstable disturbances in a Stokes layer on a surface with positive curvature have the form

$$(\psi, \phi) = \left(\sum_{n=-\infty}^{\infty} \psi_{2n+1}(\eta) e^{i(2n+1)\tau}, \quad \sum_{n=-\infty}^{\infty} \phi_{2n}(\eta) e^{2in\tau} \right),$$

and the results obtained here also have this structure, as indicated by the neutral curve of T as a function of axial wavenumber a , in figure 2. However, our results also showed that the disturbance structure for which $\psi(\eta, \tau)$ contains only even harmonics in time, as in Seminara & Hall (1976), also appears in the neutral curve but not near critical conditions.

There is a well-defined critical value of $T = T_c = 5964.03$ with corresponding $a = a_c = 1.9115$. This value for T_c leads to the asymptotic result that the solution of the original centripetal system (2.15) has the property that $R_c \sim 77.2\sqrt{H}$ for large H . This relationship is shown on figure 3 together with the results of computations on the full system (2.15). It is seen that the asymptotic result is surprisingly good over a wide range of cylinder radii and is an accurate predictor of when our flow is likely to be unstable to axially periodic centripetal modes. The amalgamation of our results shown on this figure illustrates a number features that we anticipated at the outset. For sufficiently small cylinder radius the centripetal modes are likely to be the more significant and the shear modes would probably not be detected in practice. However, as the size of the cylinder grows, the onset of instability of the two modes swaps over and the shear modes now occur at a lower value of R than the centripetal instabilities. This exchange occurs when $H \approx 86$, so that for $H > 86$ there is the possibility

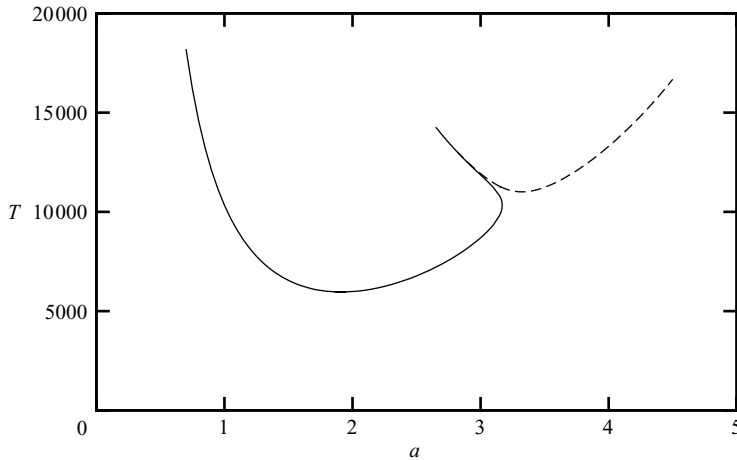


FIGURE 2. The neutral curve for centripetal instabilities, T vs. a , from the solution of the system (3.1). The solid line denotes the mode where $\phi(\psi)$ contains only even (odd) harmonics in time, as in Papageorgiou (1987); the dashed line denotes the mode where $\phi(\psi)$ contains only odd (even) harmonics in time; cf. the results of Seminara & Hall (1976).

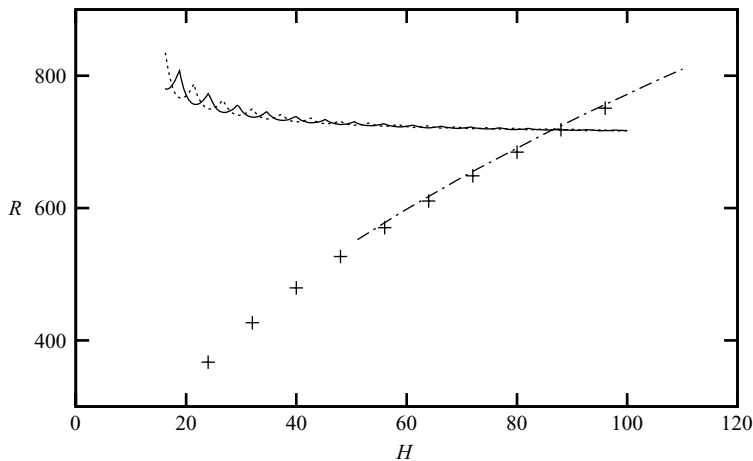


FIGURE 3. Critical conditions for instability to Stokes-layer shear modes and centripetal modes. The calculated critical conditions from the solution of the system (2.15) are shown with + signs; the asymptote, $R_c \sim 77.2\sqrt{H}$, provided by the critical conditions from (3.1) is shown by the chain line. The shear-mode critical conditions are shown by the solid line and the dotted line. Further details on the shear instabilities are given in the caption to figure 1.

that the shear modes associated with the Stokes layer would be experimentally observable.

4. Remarks

The results reported above indicate that for cylinder radii larger than 86 Stokes-layer thicknesses the shear-mode instability of a flat Stokes layer, described by BB02, determines the stability of the flow in a long torsionally oscillating cylinder. As the kinematic viscosity of water is very small, Stokes layers in water are very thin

even at quite low (dimensional) frequencies. At a frequency of 1 Hz, or 2π rads⁻¹, as used by Seminara & Hall (1976), the thickness of a Stokes layer in water is about 5.6×10^{-4} m. The requirement that $H > 86$ translates to the condition that the dimensional radius of the cylinder, r_o , is larger than about 50 mm, which would result in a quite modest-sized piece of experimental equipment. However, from a practical point of view it is the critical Reynolds number condition which puts the stronger constraint on any physical apparatus. With the amplitude of the oscillation velocity of the cylinder, V_0 , defined in terms of the angular amplitude of displacement θ_0 by $V_0 = \omega r_o \theta_0$, the requirement that Reynolds numbers above 710 be attained leads to the condition that $H\theta_0 > 710$. If θ_0 is arbitrarily set to unity, then for a frequency of 1 Hz with water as the working fluid the dimensional radius of the cylinder would need to be at least $710 \times 0.00056 \approx 0.4$ m. A smaller apparatus could be obtained by using a less viscous fluid or a higher frequency of oscillation. For these large values of H the critical conditions for the oscillating cylinder tend to those of the semi-infinite flat plate. Further, we recall the result of BB06 that the stability properties of the oscillatory channel flow are essentially those of the semi-infinite flat plate (BB02) when the channel half-width is greater than about 16. Thus here it is expected that an annulus with a gap greater than roughly 16 Stokes layer thicknesses could be used instead of the full cylinder, thereby reducing the volume of working fluid needed and also allowing the positioning of measuring equipment inside the stationary inner cylinder.

The results of BB02, more explicitly demonstrated in BB06, also point to an added bonus for experiments based on a torsionally oscillating cylinder. With piston-driven or pressure-gradient-driven flows the disturbance structure contains very-high-frequency oscillations even when the flow is laminar and stable. When the bounding surfaces drive the basic flow the disturbance structure contains far fewer large-amplitude high-frequency components, thereby allowing lower sampling rates in any measurement system.

For the model flow examined here to provide a practical apparatus capable of locating the critical conditions for the instability of essentially planar Stokes layers, two conditions must be met. Firstly the necessary truncation of an infinitely long cylinder to a finite length must not significantly change the basic flow away from the required ideal basic flow, as expressed by (2.1) or (2.12), and secondly the presence of endwalls must not affect the perturbations that are assumed to determine the stability of the ideal basic flow. In the existing literature on the stability of steady or unsteady flows both these issues are invariably intertwined and no attempt will be made to discuss them completely separately here.

It is well known that in the classical steady Taylor vortex experiments the presence of stationary endwalls causes the basic flow to be locally quite different from the target purely azimuthal flow in an infinitely long annulus. At Taylor numbers below critical, the no-slip conditions associated with the presence of the endwalls causes an imbalance: the nearby pressure field keeps the fluid particles in uniform circular motion and a secondary circulation with radial and axial velocity components results at the ends of the annulus. Both experimentally (Taylor 1923; Cole 1976) and theoretically (Blennerhassett & Hall 1979) it is known that, provided the cylinders are long enough, these secondary motions do not distort the basic flow far from the ends of the cylinders and the critical conditions for physically realizable flow are an excellent approximation to the predictions of the theory based on infinitely long cylinders. However, it is known (Benjamin & Mullin 1981) that supercritical flow in finite-length cylinders can be very different from that predicted on the basis of

infinitely long cylinders and further that the flow obtained can be very sensitive to the length of the annulus. For experiments aimed at determining the critical parameters for shear modes in a Stokes layer the operating conditions for the apparatus would have to be in the subcritical regime for any centripetal instabilities. Thus it would then be expected that any end effects associated with centripetal instabilities are avoided.

While there appears to be no existing experimental or theoretical literature indicating that a purely oscillatory flow in finite-length cylinders bounded by stationary ends will be a good approximation to the infinite-cylinder model, it is possible to argue that this is the case. As noted above, the source of the secondary motion is the mismatch of the pressure field needed to maintain circular motion and the velocity field associated with the no-slip condition on the stationary end surfaces. In the steady Taylor vortex problem this discrepancy occurs over the whole of the annular gap. However, in the purely oscillatory flow considered here, outside the Stokes layer the fluid is essentially at rest and so the no-slip condition on the endwalls imposes no extra conditions on the velocity field. It is only within the thin Stokes layer on the outer cylinder that the basic flow (2.1) does not satisfy the no-slip condition on the endwalls, and hence this is the only region where any secondary motion can be generated by pressure mismatches. As the region capable of generating any secondary flow in the oscillatory case is much smaller than in the steady case it seems likely that any additional velocity components in the oscillatory flow will be smaller than the secondary flow in the classical steady-flow case. Hence it is reasonable to expect that end effects will not distort the basic unsteady flow significantly away from the idealized flow (2.1).

The above argument is indirectly supported by the results from Blennerhassett (1976) and Smith (1975) on unsteady flow in curved pipes, where the generation of secondary flows in the cross-section of the pipe follows a similar mechanism to that causing the end-region vortices in the Taylor vortex experiment. Both these authors showed that for the secondary motion associated with the steady flow through a curved pipe to be the same size as the steady streaming generated by the unsteady component of the axial flow, the steady mean flow through the pipe must be smaller than the amplitude of the oscillatory component by a multiple of the Stokes layer thickness. The general conclusion here then is that steady secondary-flow effects coming from oscillatory driving forces are much weaker than those coming from steady driving forces. Thus, in the context of the suggested experiment with purely oscillatory forcing of the basic flow, any steady streaming coming from the endwalls of a relatively long annular region is expected to have a negligible effect on the basic flow. This view is also supported by the fact that experiments were carried out on modulated circular Couette flow (Donnelly 1964) with no reports of larger than expected secondary flows either at the ends of the cylinder or in the middle of the cylinder, where measurements are usually taken.

If it is accepted that the basic flow in a finite-length cylinder or annulus is a good approximation to the required idealized flow then there is still the question of persistence of the shear-mode instability in the finite geometry of the physical apparatus. For the case of plane Poiseuille flow, the linear critical conditions for a shear-mode instability, predicted on the basis of an infinitely wide channel (Thomas 1953; Reynolds & Potter 1967), were not accurately confirmed until the experimental work of Nishioka, Iida & Ichikawa (1975). Their experiments used a low-noise wind tunnel with a width-to-depth ratio of about 27; earlier experimental work of Kao & Park (1970) in a rectangular duct with a width-to-depth ratio of 8 produced a critical Reynolds numbers well below the theoretically predicted value. While these results are

for shear modes in steady flows they indicate that the truncation of the flow domain does not completely destroy the instability mechanism present in the theoretical model. They also show that the experimentally determined stability properties can depend on the geometric properties of the physical apparatus, which are ignored in the idealized model flow.

As mentioned at the outset, the discrepancy between the theoretical predictions of BB02 and BB06 and the available experiments, together with the inconsistencies between those experiments themselves, motivated the work described here. Our aim was to search for a system which could exhibit shear modes in an oscillatory flow but avoid the inherent difficulties presented by the long entry lengths necessary for oscillatory channel or pipe experiments. Our calculations suggest that the practical generation of shear modes could well be feasible in the torsionally oscillating geometry discussed here.

We thank the referees for their suggestions for improvements to the paper.

REFERENCES

- AKHAVAN, R., KAMM, R. D. & SHAPIRO, A. H. 1991 An investigation of transition to turbulence in bounded oscillatory Stokes flows. Part 2. Numerical simulations. *J. Fluid Mech.* **225**, 423–444.
- BATCHELOR, G. K. & GILL, A. E. 1962 Analysis of the stability of axisymmetric jets. *J. Fluid Mech.* **14**, 529–551.
- BENJAMIN, T. B. & MULLIN, T. 1981 Anomalous modes in the Taylor experiment. *Proc. R. Soc. Lond. A* **377**, 221–249.
- BLENNERHASSETT, P. J. 1976 Secondary motion and diffusion in unsteady flow in a curved pipe. PhD thesis, Department of Mathematics, Imperial College, University of London.
- BLENNERHASSETT, P. J. & BASSOM, A. P. 2002 The linear stability of flat Stokes layers. *J. Fluid Mech.* **464**, 393–410.
- BLENNERHASSETT, P. J. & BASSOM, A. P. 2006 The linear stability of high-frequency oscillatory flow in a channel. *J. Fluid Mech.* **556**, 1–25.
- BLENNERHASSETT, P. J. & HALL, P. 1979 Centrifugal instabilities of circumferential flows in finite cylinders: linear theory. *Proc. R. Soc. Lond. A* **365**, 191–207.
- BLONDEAUX, P. & SEMINARA, G. 1979 Transizione incipiente al fondo un'onda di gravità. *Rendi. Accad. Naz. Lincei* **67**, 407–417.
- BLONDEAUX, P. & VITTORI, G. 1994 Wall imperfections as a triggering mechanism for Stokes-layer transition. *J. Fluid Mech.* **264**, 107–135.
- COLE, J. A. 1976 Taylor-vortex instability and annulus-length effects. *J. Fluid Mech.* **75**, 1–15.
- COSTAMAGNA, P., VITTORI, G. & BLONDEAUX, P. 2003 Coherent structures in oscillatory boundary layers. *J. Fluid Mech.* **474**, 1–33.
- DONNELLY, R. J. 1964 Experiments on stability of viscous flow between rotating cylinders. III. enhancement of stability by modulation. *Proc. R. Soc. Lond. A* **281**, 130–139.
- FORNBERG, B. 1996 *A Practical Guide to Pseudospectral Methods*. Cambridge: Cambridge University Press.
- HALL, P. 1978 The linear stability of flat Stokes layers. *Proc. R. Soc. Lond. A* **359**, 151–166.
- KAO, T. W. & PARK, C. 1970 Experimental investigations of the stability of channel flows. Part 1. Flow of a single liquid in a rectangular channel. *J. Fluid Mech.* **43**, 145–164.
- VON KERCZEK, C. & DAVIS, S. H. 1974 Linear stability theory of oscillatory Stokes layers. *J. Fluid Mech.* **62**, 753–773.
- NISHIOKA, M., IIDA, S. & ICHIKAWA, Y. 1975 An experimental investigation of the stability of plane Poiseuille flow. *J. Fluid Mech.* **72**, 731–751.
- PAPAGEORGIOU, D. 1987 Stability of unsteady viscous flow in a curved pipe. *J. Fluid Mech.* **182**, 209–233.
- REYNOLDS, W. C. & POTTER, M. C. 1967 Finite-amplitude instability of parallel shear flows. *J. Fluid Mech.* **27**, 465–492.

- RILEY, P. J. & LAURENCE, R. L. 1976 Linear stability of modulated Couette flow. *J. Fluid Mech.* **75**, 625–646.
- SEMINARA, G. & HALL, P. 1976 Centrifugal instability of a Stokes layer: linear theory. *Proc. R. Soc. Lond. A* **350**, 299–316.
- SMITH, F. T. 1975 Pulsatile flow in curved pipes. *J. Fluid Mech.* **71**, 15–42.
- SPALART, P. R. & BALDWIN, B. S. 1988 Direct simulation of a turbulent oscillating boundary layer. In *Turbulent Shear Flows 6* (ed. J. André, J. Cousteix, F. Durst, B. Launder, F. Schmidt & J. Whitelaw). Springer.
- TAYLOR, G. I. 1923 Stability of a viscous liquid contained between two rotating cylinders. *Phil. Trans. R. Soc. Lond. A* **223**, 289–343.
- THOMAS, L. H. 1953 The stability of plane Poiseuille flow. *Phys. Rev.* **91**, 780–783.
- TREFETHEN, L. N. 2000 *Spectral Methods in MATLAB*. Philadelphia, PA: SIAM.
- VERZICCO, R. & VITTORI, G. 1996 Direct simulation of transition in Stokes boundary layers. *Phys. Fluids* **8**, 1341–1343.
- VITTORI, G. & VERZICCO, R. 1998 Direct simulation of transition in an oscillatory boundary layer. *J. Fluid Mech.* **371**, 202–232.
- WU, X. 1992 The nonlinear evolution of high-frequency resonant-triad waves in an oscillatory Stokes layer at high Reynolds number. *J. Fluid Mech.* **245**, 553–597.
- YANG, W. H. & YIH, C.-S. 1977 Stability of time-periodic flows in a circular pipe. *J. Fluid Mech.* **82**, 497–505.